

Long Term X-ray Variability in GX13+1: Energy Dependent Periodic Modulation

Robin H.D. Corbet¹

*Laboratory for High Energy Astrophysics, Code 662,
NASA/Goddard Space Flight Center, Greenbelt, MD 20771*

corbet@gsfc.nasa.gov

ABSTRACT

A search is made for periodic modulation in the X-ray flux from the low mass X-ray binary GX13+1 using Rossi X-ray Timing Explorer All Sky Monitor data collected over a period of almost seven years. From a filtered data set, which excludes measurements with exceptionally large error bars and so maximizes signal to noise, modulation is found at a period of 24.065 ± 0.018 days. The modulation is most clearly detectable at high energies (5 - 12 keV). Spectral changes are revealed as a modulation in hardness ratio on the 24 day period and there is a phase shift between the modulation in the 5 - 12 keV energy band compared to the 1.5 - 5 keV band. The high-energy spectrum of GX13+1 is unusual in displaying both emission and absorption iron line features and it is speculated that the peculiar spectral and timing properties may be connected.

Subject headings: stars: individual (GX13+1) — stars: neutron — X-rays: stars

1. Introduction

The low mass X-ray binary GX13+1 is a bright persistent source which exhibits X-ray bursts (Fleischman 1985, Matsuba et al. 1995). Counterparts have been identified in the infra-red (Naylor, Charles & Longmore 1991, Garcia et al. 1992) and radio (Grindlay & Seaquist 1986) wavebands. The X-ray and radio fluxes of GX13+1 are not correlated (Garcia et al. 1988). The IR counterpart has been seen to vary on timescales of days to tens of days but no definite orbital period has been found (e.g. Charles & Naylor 1992, Groot et al. 1996, Bandyopadhyay et al. 2002). However Groot et al. (1996) did find maximum

¹Universities Space Research Association

power at a period of 12.6 days from observations spanning 18 days. From IR spectroscopy Bandyopadhyay et al. (1999) derive a spectral type of K5III for the mass donating star. This classification implies a mass of $5M_{\odot}$ (Allen 1973) and so the mass-donor is the primary star.

GX13+1 is usually classified as an “atoll” source but has some characteristics such as the properties of its quasi-periodic oscillations (QPOs) which make it more similar to a “Z” source (Homan et al. 1998 and references therein). Schnerr et al. (2003) find that while GX13+1 follows a track in an X-ray color-color diagram on timescales of hours apparently similar to atoll sources, the count rate and power spectrum change in ways unlike any other atoll or Z source. X-ray observations of GX13+1 with CCD detectors have revealed the presence of a number of features that are attributed to iron (Ueda et al. 2001, Sidoli et al. 2002). These include an emission line near 6.4 keV, an absorption line at 7.0 keV and a deep absorption edge at 8.83 keV. Previously the only other X-ray binaries which had shown such iron absorption lines were the “superluminal” black hole candidates GRO J1655-40 (Ueda et al. 1998, Yamaoka et al. 2001) and GRS 1915+105 (Kotani et al. 2000, Lee et al. 2002).

From one year of observations with the All Sky Monitor (ASM) on board the Rossi X-ray Timing Explorer (RXTE) a modulation of the soft (1.3 - 4.8 keV) flux at a period of 24.7 ± 1 day was reported (Corbet 1996; hereafter C96). Subsequent ASM observations, however, apparently failed to find confirmation of this periodic modulation. Bandyopadhyay et al. (2002) examined 5 years worth of ASM data and concluded that while there was evidence for quasi-periodicity on a timescale of 20-30 days this modulation was not consistently present.

Here RXTE ASM light curves of GX13+1, covering just under seven years, are analyzed separated into three energy bands and different methods for dealing with variable data quality are investigated. It is concluded that the X-ray flux does indeed show a persistent modulation at a period of 24 days as initially reported.

2. Observations

The RXTE ASM (Levine et al. 1996) consists of three similar Scanning Shadow Cameras, sensitive to X-rays in an energy band of approximately 1.5-12 keV, which perform sets of 90 second pointed observations (“dwell”) so as to cover $\sim 80\%$ of the sky every ~ 90 minutes. Light curves are available in three energy bands: 1.5 to 3.0 keV (“soft”), 3.0 to 5 keV (“medium”), and 5 to 12 keV (“hard”). The Crab produces approximately 75 counts/s in the ASM over the entire energy range. Observations of blank field regions away from the Galactic center indicate that background subtraction may produce a systematic uncertainty

of about 0.1 counts/s (Remillard & Levine 1997).

Two standard ASM light curve products are routinely available - one with flux measurements from individual dwells which preserves the 90s time resolution, and one which gives averages of all dwells performed during each day. The ASM light curve of GX13+1 considered here covers approximately 6.7 years (MJD 50094 to 52536). The overall light curve of GX13+1 as obtained with the RXTE ASM is shown in Figure 1. The mean flux for the entire ASM energy range is 23 counts/s and no long term trend is obvious from the full energy-range light curve.

In C96 it was reported that the overall flux level of GX13+1 was anti-correlated with the hardness ratio. However, further investigation suggests that the major contribution to this apparent effect is gain changes in two of the three SSCs that comprise the ASM. These instrumental effects cause slow drifts in hardness ratios dependent on source spectrum with only sources with spectra identical to the Crab showing no change (Remillard private communication). A change in the channel definitions used to define the three energy bands also occurred at MJD 51548.625. This can give discontinuous jumps in the count rates in different energy bands again dependent on source spectrum. These two instrumental effects can both be seen in Figure 1. The approximately linear trends in the soft and medium energy bands give exactly the apparent hardness-ratio/intensity correlation reported in C96. The anti-correlation reported in C96 is thus at least primarily an instrumental artifact. In order to remove these trends from the lower energy bands which, in addition to giving apparent hardness ratio changes, result in spurious low-frequency power in a periodogram, the low and medium energy bands were corrected by fitting two linear trends to the light curves before and after MJD 51548 and subtracting these. The high energy light curve does not have an obvious trend and so no correction was needed.

3. Analysis and Results

To investigate long term flux variability it is often convenient to use the daily averaged ASM light curves rather than the dwell light curves. The error on these flux measurements can vary significantly due to, for example, the different number of dwells covering a source from day to day. The errors on flux measurements in individual dwells can also vary depending on factors such as the location of the source in each SSC's field of view, proximity to the position of the Sun, and the number and brightness of other sources in the field of view. When searching for periodic modulation in faint sources, for example, it can thus be advantageous to weight data points contributions to a power spectrum. In weak sources this weighting may reveal periodic modulation not otherwise easily detectable (e.g. Corbet,

Finley & Peele 1999, Corbet et al. 1999). However, this procedure is not appropriate if the variations in source flux are significantly larger than typical data point errors. For the full energy range daily averaged light curve of GX13+1 the standard deviation of the data points is 2.8 counts/s and the mean error on measurements is 0.7 counts/s. A simple direct weighting of all data points may thus not be appropriate for an analysis of GX13+1. The light curve does, however, contain some points with exceptionally large error bars because, for example, the points were obtained with only a very small number of dwells or the observations were obtained when the source was at a small angular distance from the Sun. Another simple technique was therefore considered to improve signal to noise in period searches. While the data contributions to the power spectrum are not weighted, some points with errors larger than an arbitrary value are completely excluded from the calculation of the power spectrum. How this arbitrary value is chosen is discussed below.

A further complication in weighting the data points is that the variation in the number of dwells per day is significantly non-random. The number of ASM observations made per day of GX13+1 was investigated and a very strong modulation at a period of 52.6 days was found (Figure 2). This periodicity is also found in the size of the error bars on the daily averaged flux measurements. This 52.6 day periodicity is probably linked to the precession period of RXTE’s orbit. Note that, even if unweighted techniques are used to extract power spectra, if the dwell light curve is used instead of the daily averaged light curve, then a similar weighting will effectively result.

In order to compare these different techniques for searching for periodic signals in the variable quality ASM data the effects of weighting and screening the data were investigated. In Figure 3 power spectra of the light curve of GX13+1 calculated in five different ways are shown. The techniques employed were:

- (a) using unweighted daily averages
- (b) weighted daily averages
- (c) unweighted daily averages with points with large error bars removed
- (d) weighted dwell data
- (e) unweighted dwell data

It can be seen that the unweighted procedure (a) shows a peak at near 24 days that is stronger compared to the weighted procedure (b). This peak strongly increases in significance when the points with large error bars are excluded (c). The power spectra obtained from the dwell data (d and e) show similar shapes to the weighted power spectrum with the weighted dwell data (d) almost identical to (b).

To obtain the screened unweighted power spectrum (c) data points were removed based on the size of the error bars and the power spectrum calculated. This technique is based

on the assumption that the peak exhibited in the unweighted power spectrum arises from a real modulation present in the data and that the parameters of this modulation can best be measured by utilizing a subset of the data which gives the highest overall signal to noise ratio. The filtering procedure was repeated with different data exclusion thresholds until the maximum ratio of signal peak at ~ 24 days to average power was obtained. The distribution of error bar sizes is shown in Figure 4 with the optimum screening threshold of an error of 1.4 counts/s marked. The peak of the error bar distribution is at approximately 0.4 cts/s which is considerably less than the mean error of 0.7 cts/s noted above which reflects the contribution of an extended tail on the distribution. It was found that only a relatively small number of points had to be excluded (8.2% of the original 1897 points). These excluded points all come from the extended tail and the “core” of the data is completely included. Thus, the presence of a strong peak at 24 days is unlikely to be an artifact of this screening procedure.

The power spectra of each of the ASM energy bands were next investigated individually. For each band data points were again reiteratively filtered by the size of their error bars to maximize the signal near 24 days. The fraction of data excluded was 22%, 15% and 4.5% for the soft, medium, and hard bands respectively with associated screening thresholds were 0.5, 0.5 and 1.0 counts/s. For comparison the mean and distribution peak of the errors in each band were: 0.4 and 0.19 (soft), 0.35 and 0.17 (medium), and 0.39 and 0.22 (hard). The larger fraction of data excluded for the softer bands might be due to the relatively larger effects of solar contamination at low energies as the soft energy band in particular light curve exhibits very large error bars when the GX13+1 is close to the position of the Sun. However other unknown effects might also be involved. Figure 5 shows the resulting power spectra in terms of relative power. That is, the power spectra are normalized by the mean flux in each energy band and so show relative modulation. Figure 6 shows details of the power spectra near the 24 day period but plotted as absolute modulation.

From Figures 5 and 6 the following conclusions can be drawn: (i) some signal is present in all three energy bands near 24 days. However, significant independent detection of the signal could only be made in the hard (5 to 12 keV) and summed energy bands. (ii) The greatest *relative* modulation occurs in the soft band (1.5 to 3 keV). There are, however, other peaks in the soft power spectrum of almost comparable size to the signal near 24 days. (iii) The greatest *absolute* modulation occurs in the hard band (5 to 12 keV).

The periodic modulation in each energy band was quantified by fitting sine waves to the light curves and the results of these fits are given in Table 1. Note that the periods derived from each energy band are all consistent within the errors with the value found from the summed energy band of 24.07 ± 0.02 days. This gives additional confidence that a real

period has been detected. This period is also consistent with the value reported in C96 of 24.7 ± 1 days. The phase of maximum flux, however, differs between the soft (1.5 to 3 keV) and medium (3 to 5 keV) energy bands (which are consistent with each other) and the hard (5 to 12 keV) band which trails by 4.8 ± 0.7 days ($\Delta\phi = 0.20 \pm 0.03$). This phase difference is also clearly seen directly in the folded light curves (Figure 7). Due, at least in part, to this energy dependent phase difference the folded hardness ratio is also seen to be modulated on the 24 day period. These folded light curves are rather smooth thus justifying the parameterization using sine wave fits.

To investigate the coherency of the modulation the width of the peak in the power spectrum was compared to that of a transform of a sine wave sampled with the same frequency as the actual data. For the peak in the transform of the summed energy bands we find a FWHM of 0.00031 day^{-1} and the peak in the periodogram of the pure sine wave has a FWHM of 0.00033 day^{-1} . The width of the power spectrum peak is thus fully consistent with coherency.

In order to further investigate the stability of the ~ 24 day period we calculated power spectra for each energy band using a sliding box to investigate subsets of the data. Figure 8 shows that while the strength of the modulation is variable all data segments for the hard and summed energy bands show some signal near 24 days. This variability, along with the problem of determining the optimal method to calculate the power spectra, has probably contributed to the previous difficulty in determining the reality and properties of the modulation in GX13+1 (Bandyopadhyay et al. 2002).

3.1. Comparison with Other Systems

In order to compare the properties of GX13+1 the RXTE ASM light curves of several other sources were also investigated. These were the ‘‘GX atoll’’ sources (Hasinger & van der Klis 1989) which are not known to be pulsars or transient black hole systems: GX3+1, GX9+1 and GX9+9. In each case power spectra were constructed from the daily averaged light curves both with and without weighting. Some sources showed smooth variations on long timescales caused by intrinsic variability rather than the ASM instrumental effects noted in Section 2. Quadratic fits were therefore subtracted from the lightcurves before the power spectra were calculated. The resulting power spectra are shown in Figure 9. In the weighted power spectra GX3+1 shows prominent peaks at 51.3 and 54.0 days. These are both close to the sampling period of 52.6 days for GX13+1. Thus these peaks may be an artifact. GX9+1 shows no significant peaks in the weighted power spectrum. GX9+9 shows peaks at 51.6 and 54.6 days which are again close to the 52.6 day sampling period for GX13+1.

In the unweighted power spectra the peaks near 52 days disappear for both GX3+1 and GX9+9. For GX9+1 a modest peak appears in the unweighted power spectrum at 59.5 days. However, when the data screening technique was employed for this source, it was found that exclusion of data actually reduced the relative height of the peak. This suggests that this peak in GX9+1 may be spurious. Thus none of the other “GX atoll” sources show the same type of timing properties in the RXTE ASM as GX13+1.

4. Discussion

Periodic modulation in X-ray binaries is known to arise from three types of underlying physical processes: neutron star rotation period, binary orbital period, and super-orbital modulation by a less clear physical mechanism (White, Nagase & Parmar 1995). Since neutron star rotation can be excluded because of the length of the period, two likely possibilities remain for GX13+1 of orbital or super-orbital modulation. The modulation found for GX13+1 is unusual with no directly comparable modulation found for other bright low mass X-ray binaries observed with the RXTE ASM.

Modulation of X-ray flux from low-mass X-ray binaries on the orbital period is only seen for high inclination systems. In only a few cases (e.g. EXO 0748-676, Wolff et al. 2002 and references therein) are eclipses seen in bright sources as the mass-donating star occults the central X-ray source. X-ray dipping is seen for a number of sources with moderate inclination. These dips are caused by vertical structure in the accretion disk and are tied to the orbital period but are irregular in their morphology and phasing. Spectral changes are typically seen during the dips with the spectrum becoming harder. For still lower inclination systems X-ray modulation on the orbital period typically cannot be seen but optical modulation may be observed (e.g. van Paradijs & McClintock 1995) as varying aspects of the X-ray heated mass-donating star are observed. In all cases modulation on the orbital period should be intrinsically coherent as it is locked to the orbital period, but deviations from strict periodicity can arise due to, for example, changes in the phase at which dipping occurs.

Super-orbital modulation has been seen in several systems with the strongest effects demonstrated by the high mass systems SMC X-1 and LMC X-4 and the intermediate mass system Her X-1 (e.g. Ogilvie & Dubus 2001). For low mass systems periodic super-orbital modulation appears to be rare and the best evidence for such modulation may come from X1820-30 which has a 172 day period (e.g. Chou & Grindlay 2001 and references therein). Since super-orbital modulation is likely not tied to an underlying good clock such as orbital modulation, but may instead be caused by a mechanism such as accretion disk precession forced by radiation pressure (e.g. Ogilvie & Dubus 2001 and references therein), modulation

may have low coherence. In Cyg X-2, which initially appeared to show a “clean” 78 day super-orbital periodicity (Wijnands, Kuulkers, & Smale 1996), the modulation was later found to be more complex with the excursion times between X-ray minima characterized as a series of integer multiples of the 9.8 binary orbital period (Boyd & Smale 2001).

If the modulation that is observed in GX13+1 is orbital in origin then a requirement is that the mass-donating star must not overfill the predicted Roche lobe size. Bandyopadhyay et al. (1999) find that a mass donor of spectral type K5III, as found from their IR spectroscopy, would fill the Roche lobe if the orbital period is about 25 days. If this spectral type is correct then it implies that the modulation observed would have to be orbital in nature.

The folded light curves (Figure 7) show a smooth modulation over the entire 24 day period. This indicates that the flux is being affected at all phases rather than the periodicity being caused by, for example, a sharp eclipse or dips restricted to a limited phase range. Although Accretion Disk Corona (ADC) sources, where the central X-ray source is not observed directly, can exhibit rather broad modulation the ADC sources have low X-ray luminosities and so are unlike GX13+1 which is estimated to have a luminosity of $4 - 6 \times 10^{37} \text{ (d/7 kpc)}^2 \text{ ergs s}^{-1}$ (1 - 20 keV, Matsuba et al. 1995).

The mechanism for the periodic modulation in GX13+1 is unclear. However, the “cleaner” modulation observed in the hard ASM energy band may be related to the unusual high energy features reported by Ueda et al. (2001) and Sidoli et al. (2002). The periodic modulation might be caused by material located in different parts of the binary system, such as different parts of accretion disk structure, at different energies. Note that Smith, Heindl, & Swank (2002) find from monitoring observations with the RXTE Proportional Counter Array orbital periods of 12.7 and 18.5 days for the black hole candidates 1E 1740.7-2942 and GRS 1758-258. Thus the presence of a long orbital period for GX13+1 may be another common factor, along with the iron spectral features, between GX13+1 and some black hole systems.

It is noted that Schnerr et al. (2003) interpret their unusual timing and spectral results for GX13+1 as showing the presence of an additional source of hard variable emission. This component could plausibly be identified with the periodic component of the flux that is seen most clearly in the hard band with the RXTE ASM. Schnerr et al. (2003) propose that this hard component might come from a jet and that variability could be caused by precession of the jet or to variations in jet activity itself. However, the periodicity seen in the hard component suggests that precession is unlikely to drive this variability. However, variable occultation of part of the jet by, for example, structure in the accretion disk could account for the variability if the system inclination is sufficiently high.

It may be that a portion of the hard flux does originate in a physically separate region of the system such as a jet, while softer emission comes from the inner accretion disk and/or the surface of the neutron star. If so, this could account for the different timing properties of GX13+1 found at different energies.

5. Conclusion

The X-ray light curve of GX13+1 shows strong evidence for the presence of a periodicity near 24 days with modulation properties that are energy dependent. The most likely origin for this is some type of orbital modulation if the mass donor is a Roche-lobe filling K5III star.

Because of the unusual nature of this modulation and the somewhat non-standard technique used to maximize the signal in the ASM data it would be desirable to confirm the 24 day period through other observations and determine whether the modulation is present at other wavelengths. Unfortunately no other high-quality long term observations appear to exist. Although GX13+1 was observed by the all-sky monitors on both Ariel V and Vela 5 the sensitivity of these experiments was significantly less than that of the RXTE ASM. The Ginga all-sky monitor, which was more sensitive than the Ariel V and Vela 5 instruments, did not include GX13+1 in the objects for which light curves were produced (S. Kitamoto, private communication). Infra-red light curves have been obtained by several groups (Charles & Naylor 1992, Groot et al. 1996, Wachter 1996, Bandyopadhyay et al. 2002). While these show modulations on timescales of tens of days, which could be consistent with a 24 day period, the observations do not cover sufficient durations to demonstrate whether the 24 day period is also exhibited in the infra-red.

The best prospect for confirmation of the 24 day period may come from further RXTE observations. If the RXTE ASM continues to operate for at least a few more years then the additional observations obtained will form a statistically independent data set that can be investigated for the presence of the 24 day period.

Additional constraints on models that could account for the periodic modulation may come from an investigation of whether the high energy spectral features also vary on the 24 day period. Extended IR observations would be valuable as they may show whether the 24 day period exists at these wavelengths and so constrain the system inclination.

I thank R.A. Remillard for useful comments on the properties of the RXTE ASM and S. Kitamoto for information on the Ginga ASM.

REFERENCES

- Allen, C.W., 1973, “Astrophysical Quantities”, Athlone Press
- Bandyopadhyay, R. M., Shahbaz, T., Charles, P. A., & Naylor, T., 1999, MNRAS, 306, 417
- Bandyopadhyay, R.M., Charles, P.A., Shahbaz, T., & Wagner, R.M., 2002, ApJ, 570, 793
- Bradt, H.V., Rothschild, R.E., & Swank, J.H., 1993, A&AS, 97, 355
- Charles, P.A., & Naylor, T., 1992, MNRAS, 225, 6P
- Chou, Y. & Grindlay, J.E., 2001, ApJ, 563, 934
- Corbet, R., 1996, IAUC 6508 (C96)
- Corbet, R.H.D., Finley, J.P., & Peele, A.G., 1999, ApJ, 511, 876
- Corbet, R.H.D., Marshall, F.E., Peele, A.G., & Takeshima, T., 1999, ApJ, 517, 956
- Fleischman, J.R., 1985, A&A, 153, 106
- Garcia, M. R., Grindlay, J. E., Molnar, L. A., Stella, L., White, N. E., & Seaquist, E. R., 1988, ApJ, 328, 552
- Garcia, M.R., Grindlay, J.E., Bailyn, C.D., Pipher, J.L., Shure, M.A., & Woodward, C.E., 1992, ApJ, 103, 1325
- Grindlay, J.E. & Seaquist, E.R., 1986, ApJ, 310, 172
- Groot, P.J., van der Klis, M., van Paradijs, J., Augusteijn, T. & Berger, 1996, in “Cataclysmic Variables and Related Objects”, ed. A. Evans & J.H. Wood, p. 367
- Hasinger, G. & van der Klis, M., 1989, A&A, 225, 79
- Homan, J., van der Klis, M., Wijnands, R., Vaughan, B., & Kuulkers, E., 1998, ApJ, 499, L41
- Kotani, T., Ebisawa, K., Dotani, T., Inoue, H., Nagase, F., Tanaka, Y., & Ueda, Y., 2000, ApJ, 539, 413
- Lee, J.C., Reynolds, C.S., Remillard, R., Schulz, N.S., Blackman, E.G., & Fabian, A.C., 2002, ApJ, 567, 1102
- Levine, A.M., Bradt, N., Cui, W., Jernigan, J.G., Morgan, E.H., Remillard, R., Shirey, R.E., & Smith, D.A., 1996, ApJ, 469, L33
- Matsuba, E., Dotani, T., Mitsuda, K., Asai, K., Lewin, W.H.G., van Paradijs, J., & van der Klis, M., 1995, PASJ, 47, 575
- Naylor, T., Charles, P.A., & Longmore, 1991, MNRAS, 252, 203
- Ogilvie, G.I. & Dubus, G., 2001, MNRAS, 320, 485

- Schnerr, R.S., Reerink, T., van der Klis, M., Homan, J., Méndez, M., Fender, R.P., & Kuulkers, E., 2003, *A&A*, in press.
- Sidoli, L., Parmar, A. N., Oosterbroek, T., & Lumb, D., 2002, *A&A*, 385, 940
- Smith, D.M., Heindl, W.A., & Swank, J.H., *ApJ*, 578, L129
- Stella, L., White, N.E., & Taylor, B.G., 1985, *ESA SP-236*, p. 125
- Ueda, Y., Inoue, H., Tanaka, Y., Ebisawa, K., Nagase, F., Kotani, T., & Gehrels, N., 1998, *ApJ*, 492, 782 (erratum 500, 1069)
- Ueda, Y., Asai, K., Yamaoka, K., Dotani, T., & Inoue, H., 2001, *ApJ*, 556, L87
- van Paradijs, J. & McClintock, J.E, 1995, in “X-ray Binaries”, p. 58, ed. W.H.G. Lewin, J. van Paradijs, & E.P.J. van den Heuvel, Cambridge University Press.
- Wachter, S., 1996, *BAAS*, 189, 4404
- White, N.E., Nagase, F., & Parmar, A.N., 1995, in “X-ray Binaries”, p. 1, ed. W.H.G. Lewin, J. van Paradijs, & E.P.J. van den Heuvel, Cambridge University Press.
- Wijnands, R.A.D., Kuulkers, E., & Smale, A.P., 1996, *ApJ*, 473, L45
- Wolff, M.T., Hertz, P., Wood, K.S., Ray, P.S., & Bandyopadhyay, R.M., 2002, *ApJ*, 575, 348
- Yamaoka, K., Ueda, Y., Inoue, H., Nagase, F., Ebisawa, K., Kotani, T., Tanaka, Y., & Zhang, S.N., 2001, *PASJ*, 53, 179

Figure Captions

Fig. 1.— The RXTE ASM light curve of GX13+1 divided into three energy bands and the summed light curve. The linear trends and the discontinuities in the low- and medium-energy light curves at MJD 51548.6 are due to instrumental effects. All light curves are smoothed and rebinned versions of the standard one day averaged light curves.

Fig. 2.— Lower panel: Number of ASM observations (“dwells”) per day of GX13+1. Upper panel: power spectrum of the curve shown in the lower panel. The strongest power is found at a period of 52.6 days.

Fig. 3.— Power spectra of the ASM light curve of GX13+1 obtained in five different ways. (a) Unweighted power spectrum of daily average light curve; (b) Weighted power spectrum of daily average light curve; (c) Unweighted power spectrum of daily average light curve with data filtered to exclude points with large error bars; (d) Weighted power spectrum of individual dwell data; (e) Unweighted power spectrum of individual dwell data.

Fig. 4.— Distribution of error bar sizes from the daily averaged ASM light curve. The vertical dashed line shows where the cut was made which maximizes the relative strength of the signal near a period of 24 days in the power spectrum.

Fig. 5.— Power spectra of the ASM light curve of GX13+1 divided into three energy bands. In each case data screening was performed to maximize the signal at a period near 24 days. The power is normalized to the average count rate in each energy band and is in units of “percentage modulation squared”, i.e. the Fourier amplitude is divided by the mean flux and the square of this quantity plotted.

Fig. 6.— Details of the power spectra of the ASM light curve of GX13+1 near the 24 day period (equivalent to a frequency of approximately 0.042 day^{-1}). For this plot the power is *not* normalized to the average count rate.

Fig. 7.— Folded ASM light curves of GX13+1 and hardness ratio (5 - 12 keV/ 1.5 - 5 keV). Two cycles are shown for clarity. The orbital period and epoch of maximum are taken from the sine wave fit to the hard band alone (Table 1).

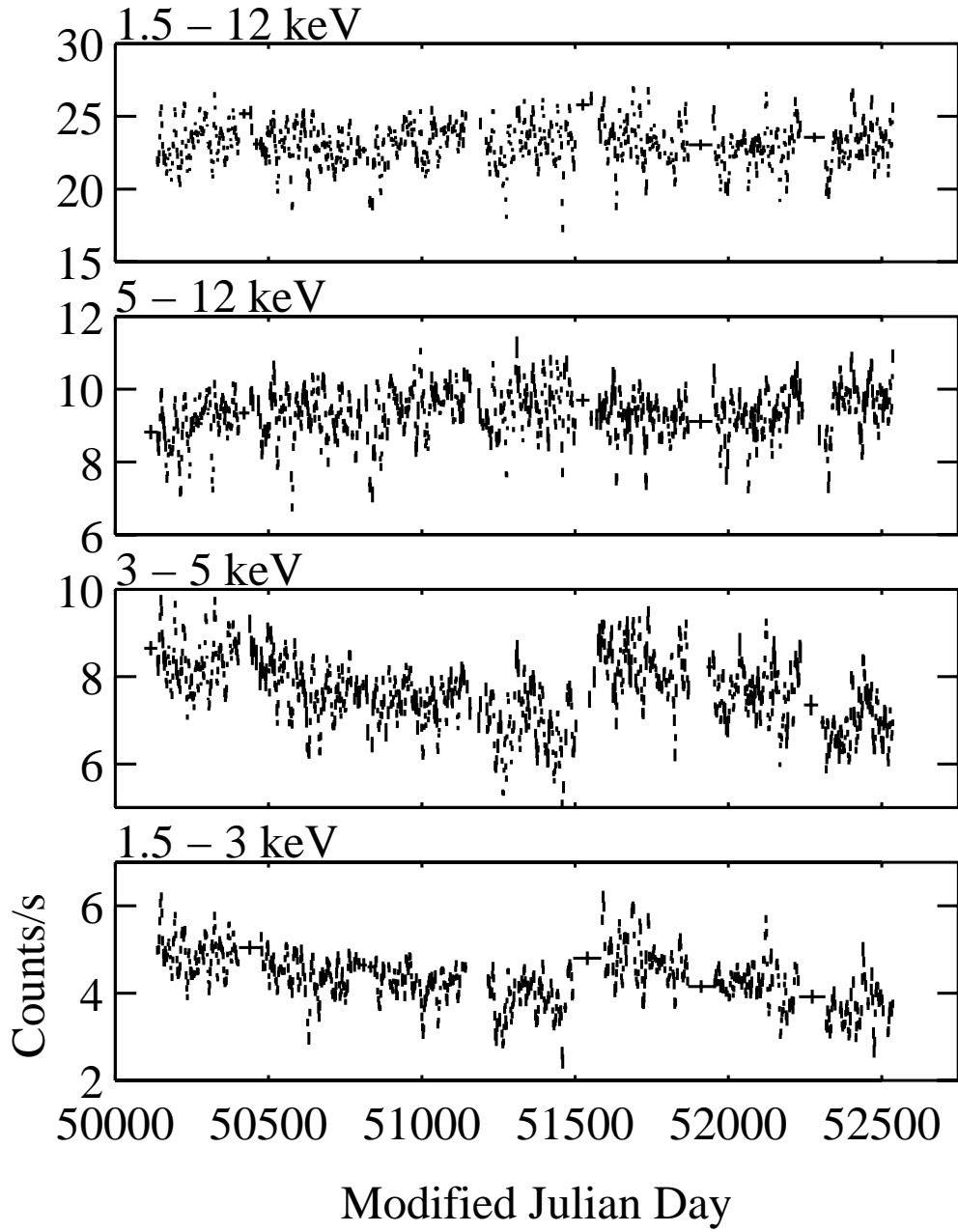
Fig. 8.— Variations in power spectra of GX13+1 as a function of time separated by energy. In each power spectrum $2 \frac{1}{3}$ years worth of data were analyzed with the start time of the power spectrum increased by 6 months between each power spectrum. The individual power spectra for each energy band are thus not statistically independent. The plots for the energy separated power spectra are all on the same scale but the summed energy band power spectra use a different y axis scale. The vertical dashed lines indicate the proposed

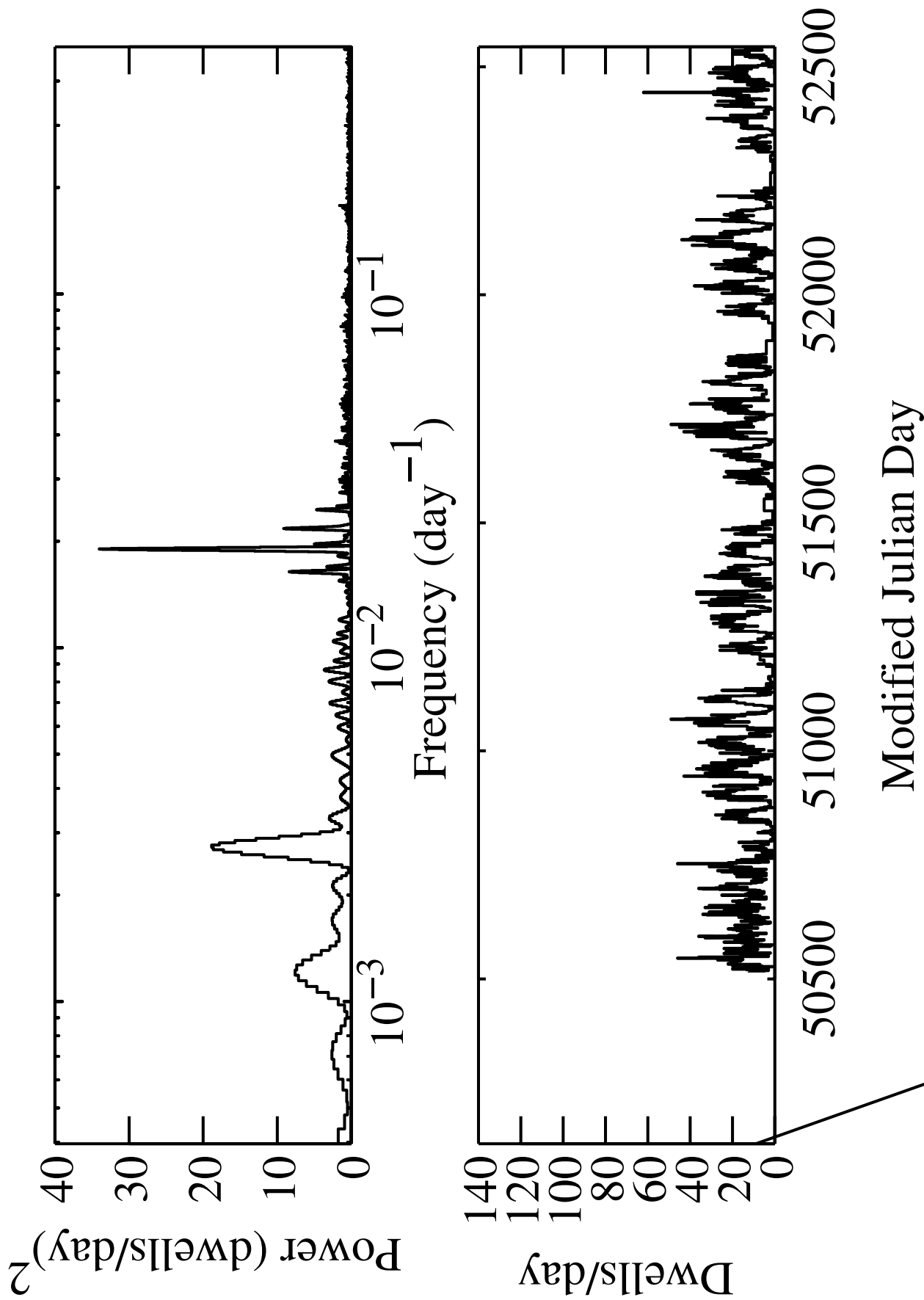
24.07 day period. Time intervals correspond, from bottom panels to top, to MJDs of: 50137 – 50989, 50319 – 51172, 50502 – 51354, 50685 – 51537, 50867 – 51719, 51050 – 51902, 51233 – 52085, 51415 – 52267

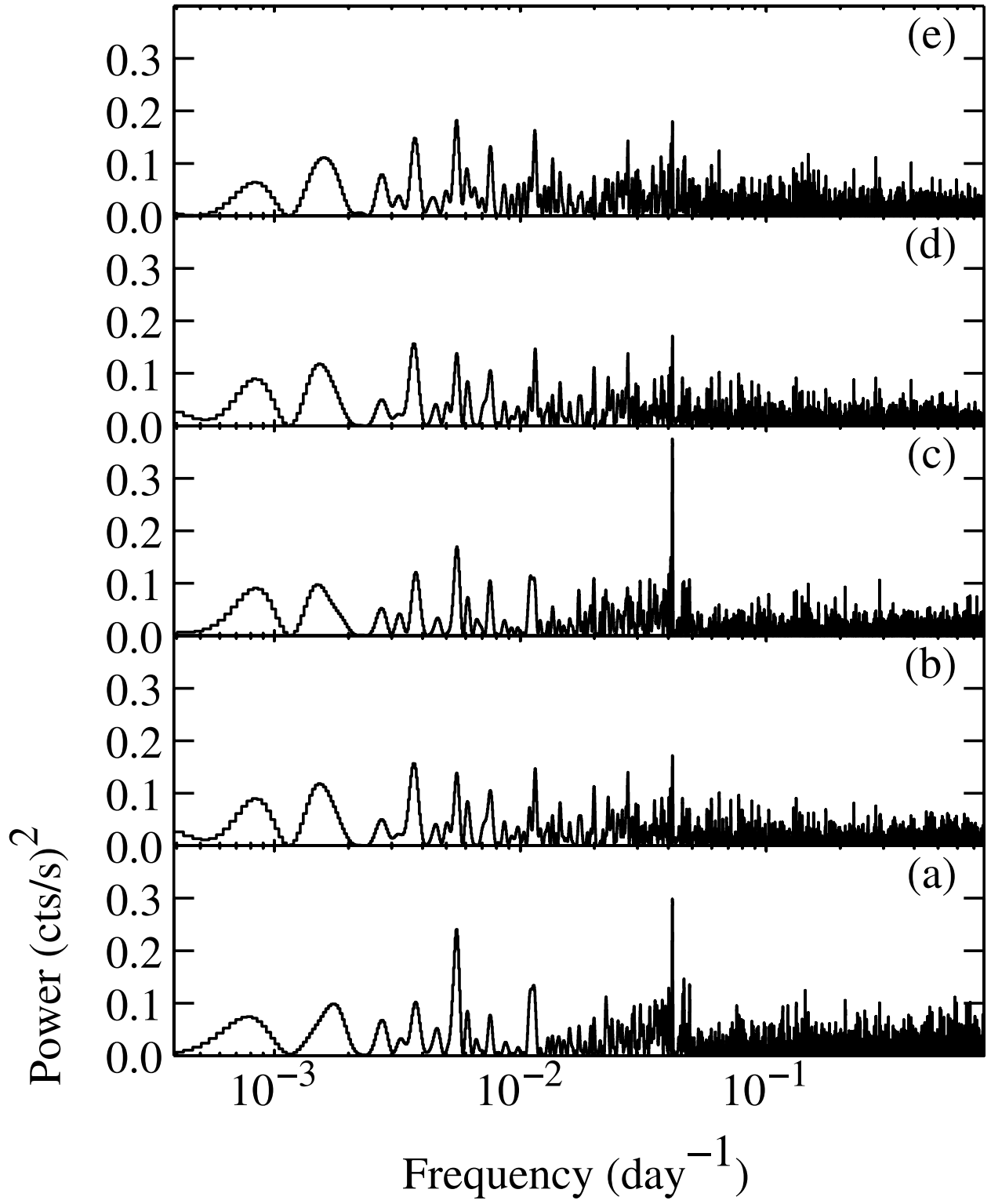
Fig. 9.— Power spectra of RXTE ASM light curves of: (a) GX3+1, (b) GX9+1, (c) GX9+9, and (d) GX13+1. Both weighted (left) and unweighted (right) power spectra are shown. In all cases light curves were prewhitened by subtraction of a quadratic fit.

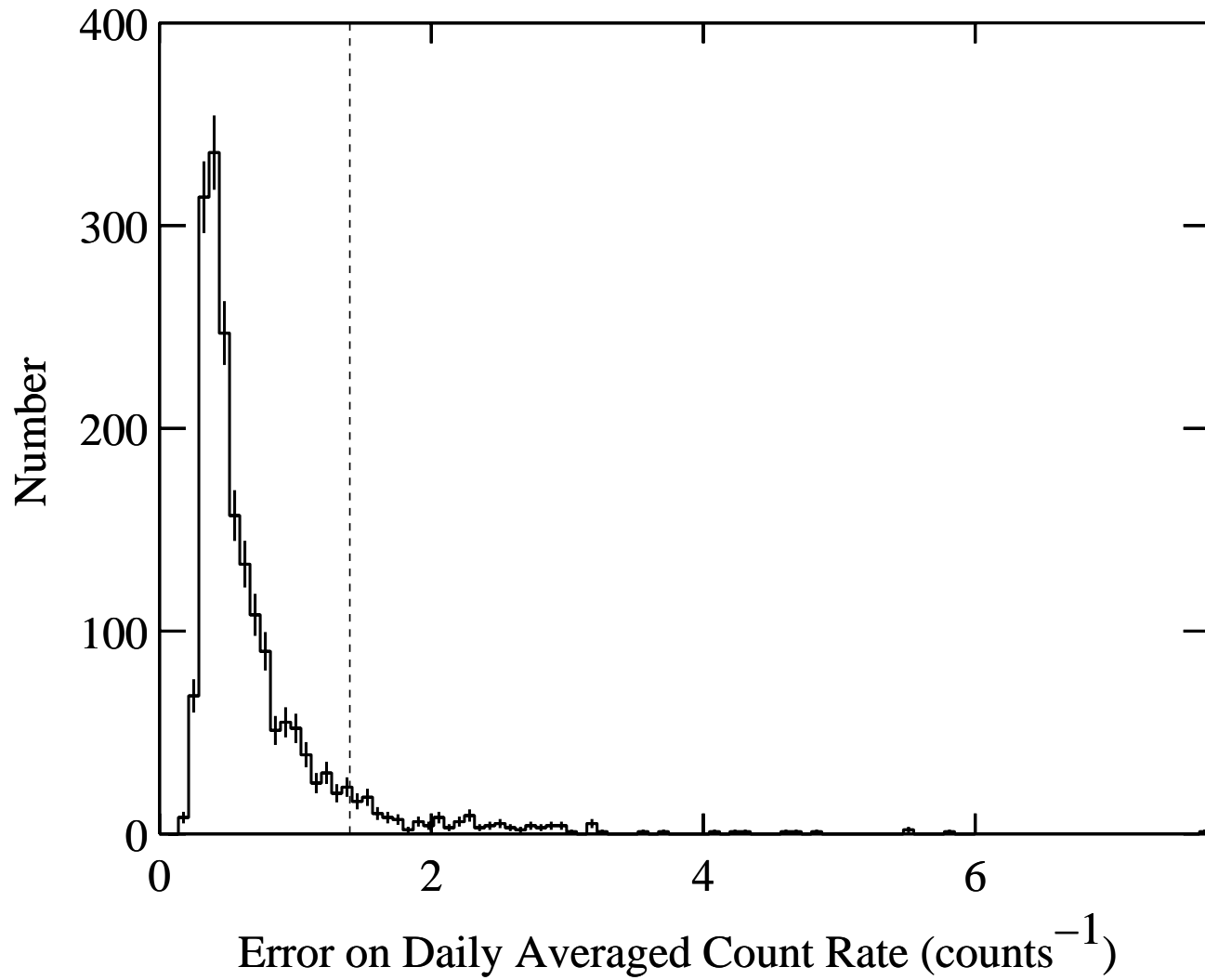
Table 1: Sine Wave Fits to GX13+1 ASM Light Curves

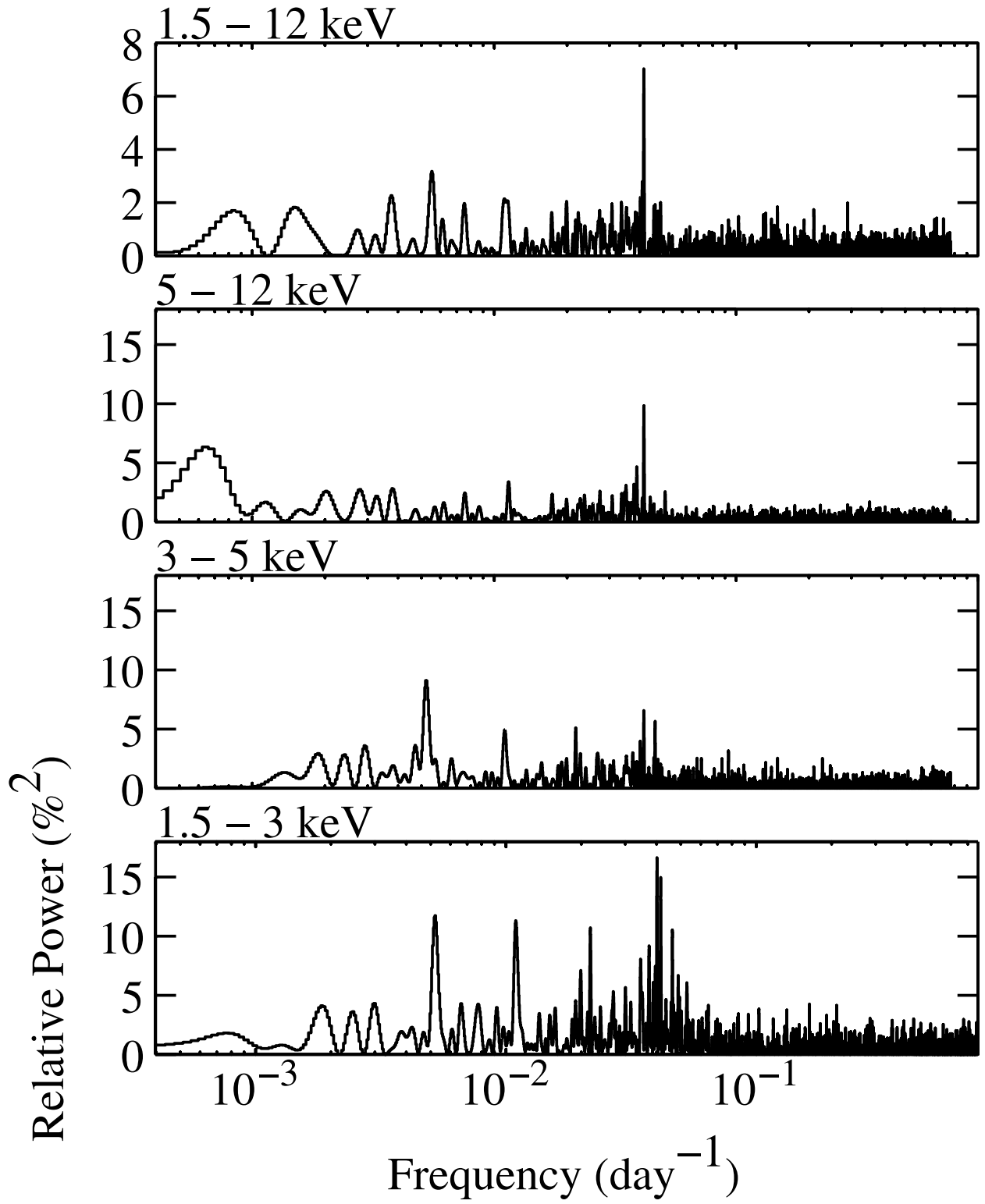
Energy Band (keV)	Mean Count Rate (cts/s)	Amplitude (cts/s)	Amplitude (%)	Period (days)	T_{max} (MJD)
1.5 – 3	4.38 ± 0.01	0.16 ± 0.02	3.7	24.063 ± 0.019	51112.2 ± 0.6
3 – 5	7.64 ± 0.02	0.19 ± 0.03	2.5	24.062 ± 0.024	51112.5 ± 0.7
5 – 12	9.35 ± 0.02	0.30 ± 0.03	3.2	24.058 ± 0.015	51117.1 ± 0.5
1.5 – 12	23.10 ± 0.06	0.61 ± 0.08	2.7	24.065 ± 0.018	51115.3 ± 0.5

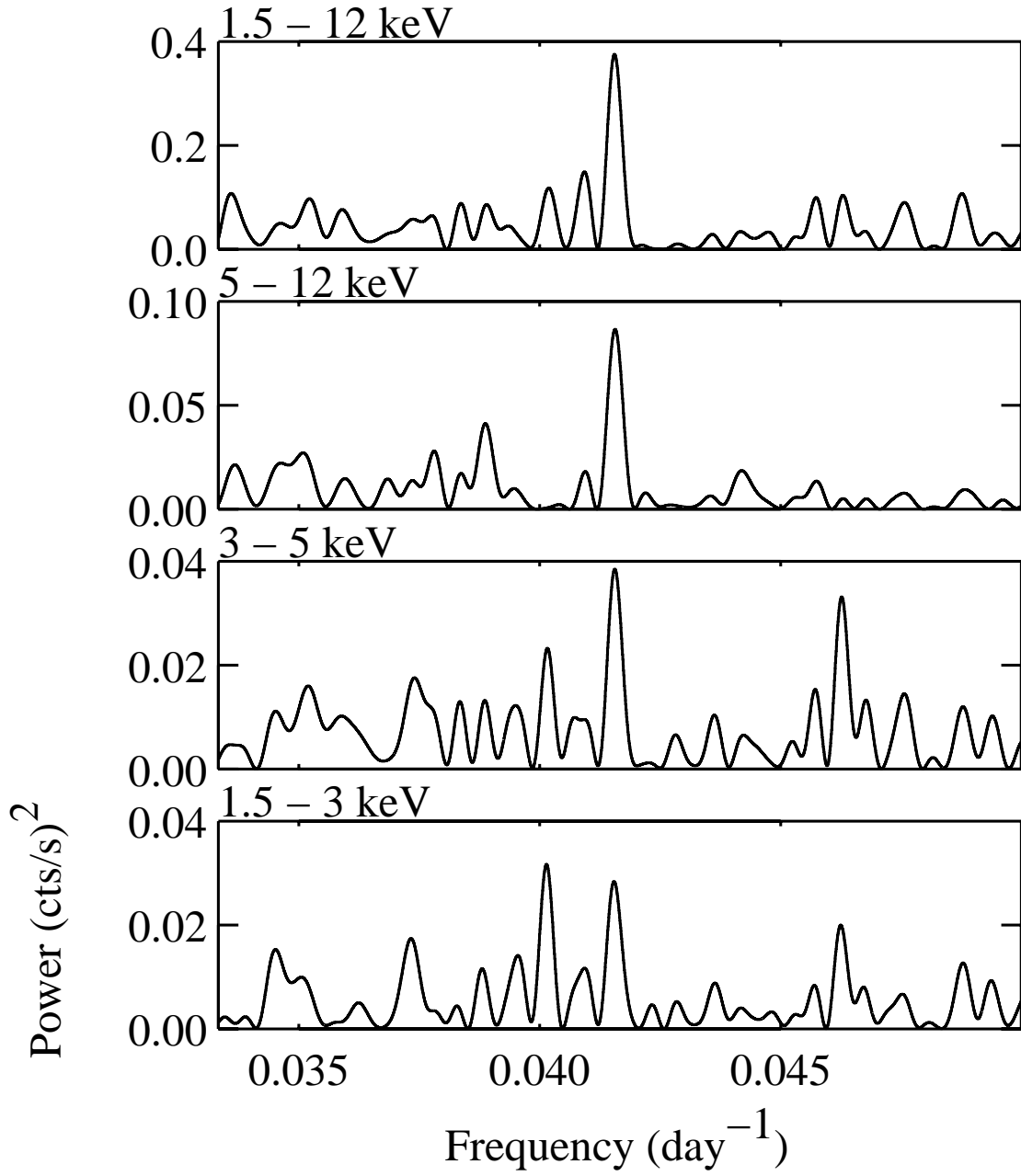


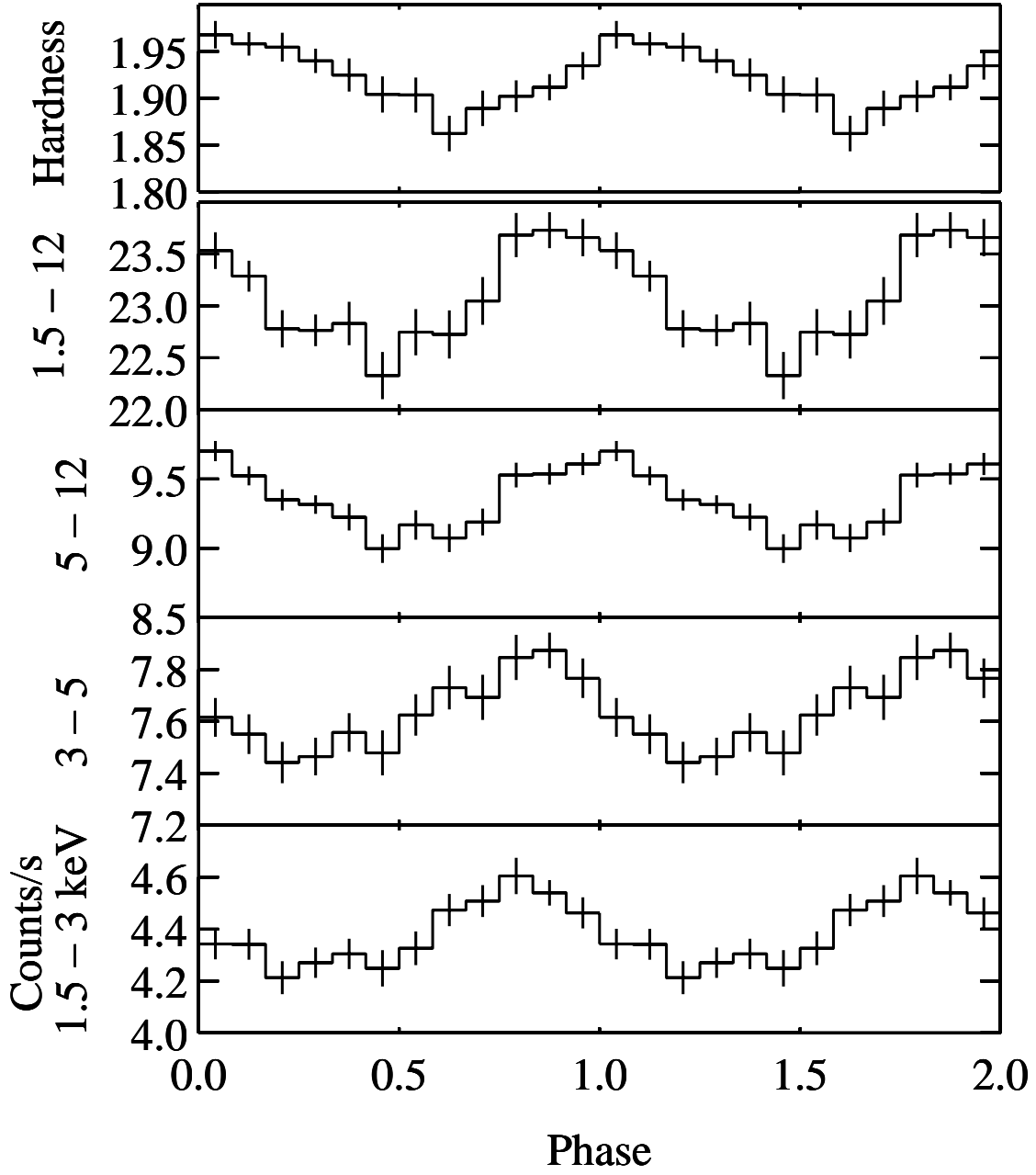


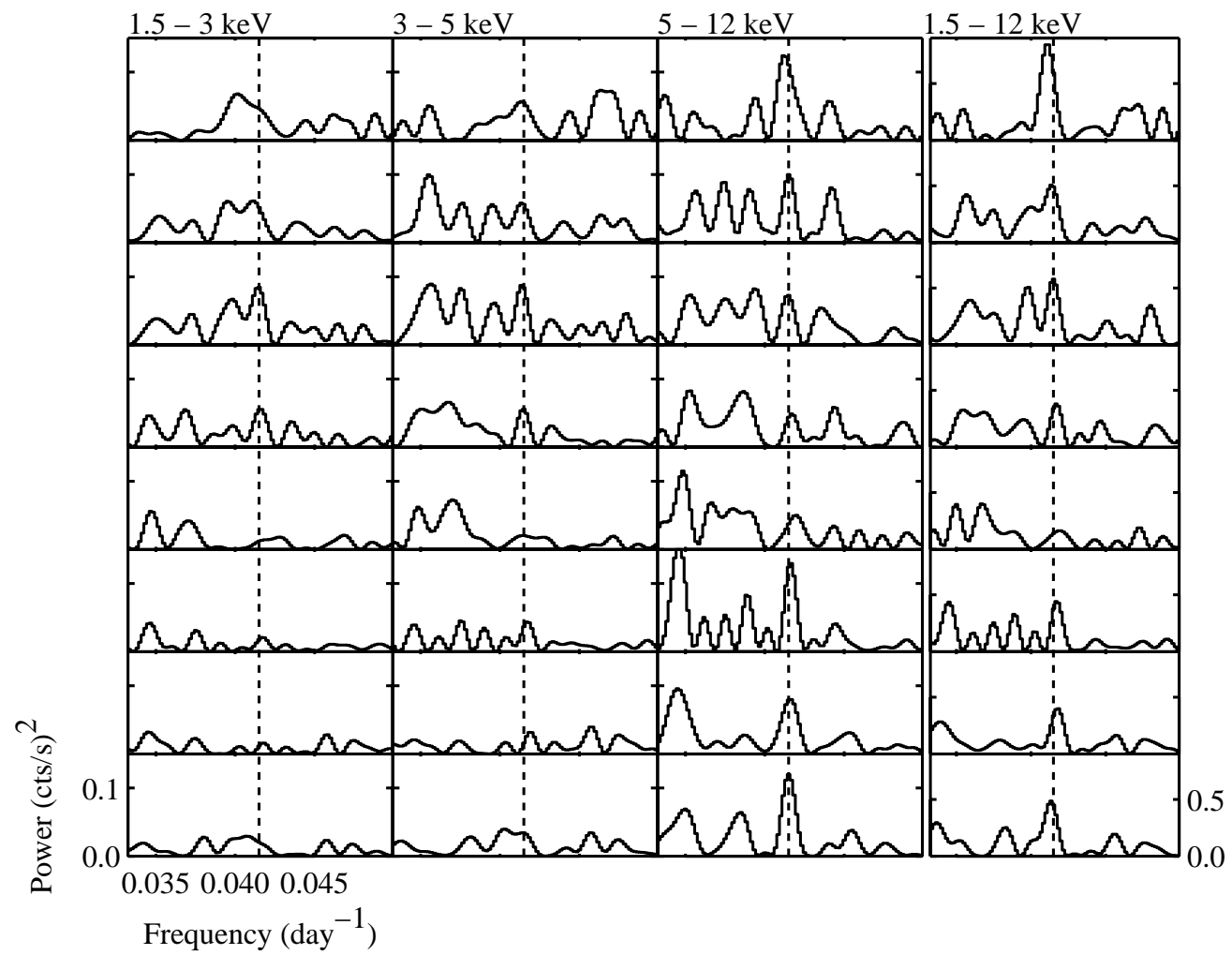


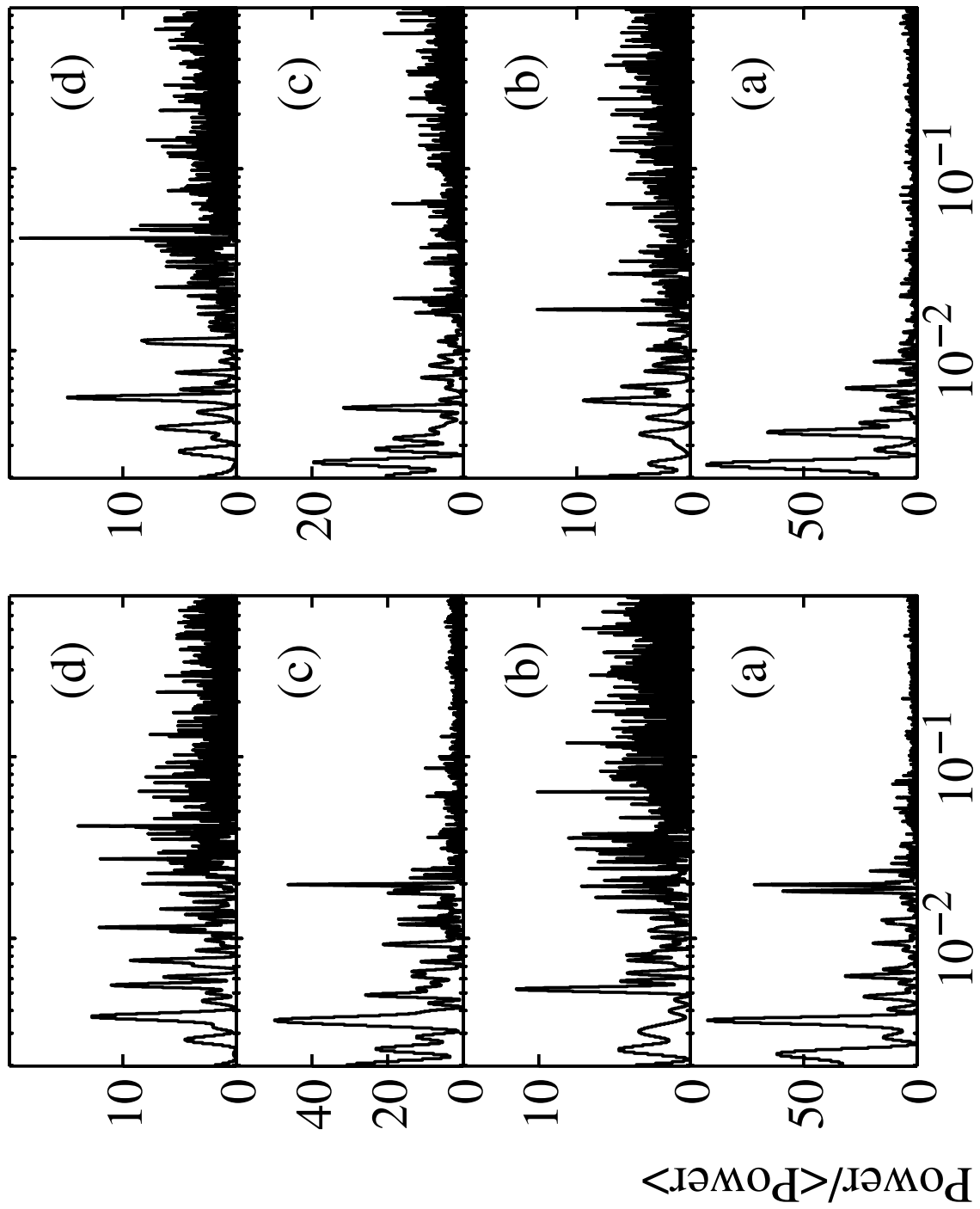












Frequency (day^{-1})